Age-related Immune-Stromal Networks Inhibit Response to Regenerative Immunotherapies

Jin Han[1], Christopher Cherry[1], Joscelyn C. Mejias[1], Anna Ruta[1], David R. Maestas Jr.[1], Alexis N. Peña[1], Helen Hieu Nguyen[1], Brenda Yang[1], Elise Gray-Gaillard[1], Natalie Rutkowski[1], Ada J. Tam[2], Elana J. Fertig[3,4,5], Franck Housseau[2], Sudipto Ganguly[2], Erika M. Moore[6], Drew M. Pardoll[2], and Jennifer H. Elisseeff[1,2,*]

[1]Translational Tissue Engineering Center, Wilmer Eye Institute and Department of Biomedical Engineering, Johns Hopkins University; Baltimore, MD, USA

[2]Bloomberg~Kimmel Institute for Cancer Immunotherapy, Sidney Kimmel Comprehensive Cancer Center, Johns Hopkins University School of Medicine; Baltimore, MD, USA

[3]Department of Biomedical Engineering and Institute for Cell Engineering, Johns Hopkins University School of Medicine; Baltimore, MD, USA

[4]Department of Oncology, Johns Hopkins University School of Medicine; Baltimore, MD, USA

[5]Department of Applied Mathematics and Statistics, Johns Hopkins University; Baltimore, MD, USA

[6]Department of Materials Science and Engineering, University of Florida; Gainesville, FL USA

*Address for correspondence: jhe@jhu.edu

Abstract

Aging is associated with immunological changes that compromise response to infections and vaccines, exacerbate inflammatory diseases and could potentially mitigate tissue repair. Even so, age-related changes to the immune response to tissue damage and regenerative medicine therapies remain unknown. Here, we characterized how aging induces immunological changes that inhibit tissue repair and therapeutic response to a clinical regenerative biological scaffold derived from extracellular matrix. Tissue signatures of inflammation and interleukin (IL)-17 signaling increased with injury and treatment in aged animals, and computational analysis uncovered dysfunctional immune-stromal cell communication. Local inhibition of type 3 immune activation using IL17-neutralizing antibodies improved healing and restored therapeutic response to the regenerative biomaterial, promoting muscle repair in older animals. These results provide insights into tissue immune dysregulation that occurs with aging that can be targeted to rejuvenate repair.

Aging is associated with decreased tissue function and a compromised response to tissue damage that leads to longer recovery and frequently dysfunctional tissue repair regardless of tissue type[1-3]. Reduced healing capacity with increasing age was recognized as early as 1932[4]. Consistent with the variability in biological signatures of aging, the variability in time required for tissue repair and the variability in resulting tissue quality increases with age in both preclinical models and patients[5-7]. Multi-omic analyses of cellular and molecular profiles of organisms over lifespan implicate changes in gene expression, metabolism, DNA methylation and epigenetic factors in age-associated pathologies including impaired wound healing[2,3]. Recovering tissue repair capacity that is lost with aging represents a significant medical challenge. While murine models of tissue repair and regeneration have brought forward transformational learnings, the vast majority of studies have been done in young mice – the equivalent of human adolescents. However, most ailments clinically affecting tissue health in humans are in the elderly demographic.

Regenerative medicine and tissue engineering approaches are designed to enhance repair and restore tissue function. While many patients needing regenerative medicine technologies are older, the influence of age-related physiological changes on regenerative medicine therapeutic responses remains unexplored. In fact, age-related changes may be, in part, related to the disappointing clinical translation and efficacy of tissue engineering technologies and should be considered in their design. The composition and phenotype of cells responding to tissue damage change with age. In skin wounds, the number of fibroblasts responding to injury is greater in older mice and the fibroblasts have reduced phenotypic heterogeneity compared to the wounds in younger counterparts[8]. In the case of muscle tissue, the number and activity of muscle stem cells decrease with age leading to sarcopenia and impaired muscle healing after injury[9]. However, the functionality of aged muscle stem cells can be restored *ex vivo* to recover healing capacity after re-injection *in vivo*, suggesting that endogenous repair capacity is retained but the aging tissue environment impedes repair[9]. Similarly, repair in the aging retina could be restored by targeting age-related epigenetic changes[10], again suggesting that regeneration capacity remains with increasing age despite decreased cell numbers and inhibitory factors.

Classical regenerative medicine strategies utilize stem cells, growth factors and biomaterials alone or in combination to promote tissue development[11]. More recently, the role of the immune system in tissue repair is being recognized as a key factor in determining healing outcomes leading to the introduction of immunomodulation as a new therapeutic modality in

regenerative medicine technology design. However, there are also numerous age-related changes that occur in the immune system that may impede a regenerative therapeutic response[12]. Age-related immune changes have been primarily studied in the context of infectious disease, chronic inflammatory conditions, vaccine efficacy and more recently cancer immunotherapy efficacy, but they may also negatively impact the response to tissue damage and regenerative medicine therapies[13]. For example, T cell numbers decrease with aging and there is a myeloid shift in the bone marrow[14,15]. Furthermore, there are composition changes in the T cell compartment with aging that include increased $CD8^+$ T cells, reduced naïve $CD4^+$ T cells, and increased effector $CD4^+$ T cells which altogether may compromise a pro-regenerative immune response and tissue repair[14].

Here, we investigated how immunological changes associated with aging impact the response to muscle injury and limit the regenerative capacity of a therapeutic biological scaffold. We show that age-related increases in hardwired chronic Interleukin (IL)-17 production by innate and adaptive elements of the immune system combined with dysfunctional stromal interactions antagonize tissue regeneration while supporting fibrosis and adipogenesis. IL17 blockade thus therapeutically reverses this age-associated impairment. Targeting age-associated immunological changes that inhibit a regenerative response may enable recovery of a therapeutic response and restoration of tissue repair capacity in older organisms.

Aging reduces type 2 immune and tissue repair responses to regenerative biomaterials

To evaluate the impact of aging on the immune response and resulting repair efficacy, we characterized the response to an extracellular matrix (ECM) biomaterial in a muscle wound in young (6 week) and old (72 week) mice (**Fig. 1a**). ECM biomaterials, derived from the matrix of different porcine and human tissue types[16], are used for tissue repair in multiple clinical indications[17,18] and are more easily delivered than cells and growth factors[19-21]. In this study, we utilized clinically available[22] ECM from porcine small intestinal submucosa (SIS) as an example ECM material to model age-related differences in response. Previous research showed that muscle repair requires a type 2 immune response with IL4 signaling[23,24] and alternatively activated macrophages. Application of an ECM biomaterial in a muscle injury further increases IL4 expression and promotes repair in part by increasing recruitment of IL-4 producing eosinophils and $CD4^+$ T helper (Th) 2 cells[25].

One week after volumetric muscle loss (VML) injury, aging significantly altered the cytokine gene expression profiles in injured tissue and with ECM treatment (**Fig. 1b**). In young animals, *Il4* gene expression increased in muscle tissue after injury with further significant increases after ECM treatment. However, *Il4* expression did not increase after injury in old mice and the level of expression after ECM treatment was significantly lower than the young animals. Instead, ECM treatment in aged mice significantly increased the expression of *Il17f* (*Il17a* gene expression was not detected in the muscle tissue of young or aged mice). Interestingly, other inflammatory genes, including *Ifnγ, Il23a*, *Il6*, *Il1b*, along with *Cdkn2a* and *S100a4*, all increased similarly in both young and old mice with injury or ECM treatment (**Extended Data Fig. 1**).

Next, using multiparametric spectral flow cytometry (**Extended Data Fig. 2**), we found injury and ECM treatment resulted in distinct changes in immune and stromal cell responses in an aging tissue environment (**Fig. 1c** and **Extended Data Fig. 3-5**). A robust cellular response to injury and ECM implant occurred in both young and aged animals but there were significant differences in the composition of the immune and stromal compartments. Specifically, the number and percentage of eosinophils in muscle tissue, a major source of regenerative type 2 response, increased in young animals with injury and ECM treatment compared to no injury controls (**Fig. 1c** and **Extended Data Fig. 4-5**). While the eosinophil counts and percentage also increased in the muscle injury of aged mice with ECM treatment (**Extended Data Fig. 4**), their percentage as a total of all $CD11b^+$ myeloid immune cells was significantly lower compared to young counterparts (p=0.0126; **Extended Data Fig. 5**). The adaptive T cell immune response to muscle injury and ECM treatment also significantly changed with age with more CD8 T cells responding to injury and ECM treatment in the aged animals compared to the CD4 and natural killer T (NKT) cell response in the young (**Extended Data Fig. 4**). The $CD45^-$ population, including fibroblasts, endothelial and other stromal cells, also significantly increased in number after ECM treatment in aged animals compared to young animals (p=0.0057; **Extended Data Fig. 4**).

The significant differences in immune cell recruitment and cytokine expression correlated with changes in tissue repair observed histologically (**Fig. 1d** and **Extended Data Fig. 6**). One week after injury and treatment, there was significant cell infiltration in both young and aged mice, with ECM treatment further increasing cellular infiltration and collagen deposition as visualized by Masson's Trichrome staining. The area of injury and ECM appeared much larger in the older animals suggesting that there was already significant repair occurring in young animals that did

not occur in the aged tissue environment. There was also excessive adipose tissue in the muscle of aged animals compared to the younger counterparts, which increased further with ECM treatment (**Fig. 1d**).

Single cell analysis reveals age-specific immune and stromal response after injury and regenerative medicine treatment

To further identify age-related signatures of injury and therapeutic response to a regenerative biomaterial therapy, we performed single cell RNA sequencing (scRNA-seq) on $CD45^{+}$-enriched cells isolated from the muscle injuries with or without ECM treatment (**Fig. 1a**). We found multiple distinct cell clusters in the merged samples (**Fig. 1e** and **Extended Data Fig. 7-9**) that included myeloid cells, T cells, granulocytes, fibroblasts, endothelial/pericytes, and skeletal muscle cells. We observed two different macrophage subtypes containing Mrc1 macrophage (Mrc1 Mc; *Mrc1*^{hi}*Ccl8*^{hi}) and Arg1 macrophage (Arg1 Mc; *Arg1*^{hi}*Mmp12*^{hi}) and detected multiple clusters in the fibroblast population consisting of generic fibroblast (Gen Fib; *Col1a1*^{hi}*Col3a1*^{hi}), Mgp fibroblast (Mgp Fib; *Mgp*^{hi}*Apod*^{hi}), and Pi16 fibroblast progenitor (Pi16 Fib; *Pi16*^{hi}*Cd34*^{hi}). Fibroblasts with high *Mgp* expression are typically defined as reticular fibroblasts[26-29], and *Pi16* is known to participate in regulating leukocyte infiltration and activation of the endothelial barrier[30]. Additionally, we identified generic myeloid cell (Gen Myl; *Adgre1*^{lo}*Ccr2*^{hi}*Cd74*^{hi}), granulocyte type 1 (Gr-1; *S100a8*^{hi}*Il1f9*^{hi}), granulocyte type 2 (Gr-2; *Ngp*^{hi}*Camp*^{hi}), T cells (*Trbc2*^{hi}), CD209 dendritic cell (CD209 DC; *Cd209a*^{hi}), a combination of endothelial cells and pericytes (Endo/Peri; *Fabp*^{hi}*Rgs*5^{hi}), and skeletal muscle cells (SMC; *Acta1*^{hi}*Myh4*^{hi}).

There were unique changes in cell clusters from ECM-treated muscle injuries in young and aged animals (**Extended Data Fig. 10**). Granulocyte cluster Gr-2, enriched with *Camp* expression, increased after injury and ECM treatment only in young animals. *Camp* is associated with early transcriptional states of neutrophils[31,32] and their cytokine and chemokine profile induces migration of eosinophils[33,34], supporting the increased eosinophil migration in young animals found by flow cytometry (**Fig. 1c** and **Extended Data Fig. 5**). The skeletal muscle cell cluster also increased with ECM treatment only in young animals, further suggesting that ECM increased myogenic activity primarily in young mice. On the other hand, the *CD209*^{hi} dendritic cell cluster, whose cytokines are known to promote Th17 phenotypes in T cells[35-38] increased with ECM only

in aged mice. Other clusters including Gr-1, Gen Myl, Mgp fib, and Endo/Peri changed with ECM treatment in a similar manner in both young and aged animals.

Aged animals exhibit impaired immune-stromal interactions required for vascularization and tissue development

Tissue repair requires removal of debris, mobilization of stem cells, vascularization, and secretion and organization of tissue-specific extracellular matrix that is coordinated through complex immune-stromal cell interactions. To further probe the differences in the young and aged tissue environment after trauma and biomaterial application, we applied Domino to model cell-cell communication patterns using the data obtained from scRNA-seq. Domino is a computational tool that identifies condition-specific intercellular signaling dynamics based on transcription factor (TF) activation, which is surmised based on regulon expression with SCENIC gene regulatory network analysis[39], along with receptor (R) and ligand (L) expression independent of cluster[40]. Domino constructs a signaling network connecting TF-R-L, which are specifically predicted to be active in the data set. TF-R connections are determined by examining correlation between R expression and TF activation scores across all cells in the data set, identifying TF-R pairings with grouped increases of expression and activation in target cell populations. R-L pairs are then determined for target receptors through the CellphoneDB2 database. In both young and old animals, a force directed diagram of the TF-R-L signaling network self-assembled into three signaling modules enriched in fibroblast, antigen processing and immune-tissue clusters (**Fig. 1f, top panel**). Each module indicates signaling pathways with similarly enriched activation in specific cell types. Increased module density and decreased connection across modules both indicate a group of highly correlated signaling patterns expressed in a specific cell population (both receptors and transcription factors). A complete list of the TFs and receptors corresponding to the activated TFs is provided in **Extended Data Fig. 11-13**.

The fibroblasts in the aged tissue appeared to lose immunological properties and the narrow localization of the activated TFs suggest reduced heterogeneity (**Fig. 1f, top panel**). The increased connectivity between fibroblast and immune-tissue modules in the young signaling network indicates some level of plasticity in signaling in young animals, and young fibroblasts appeared to respond to the signaling patterns active in immune-tissue module. In contrast, the R and TF in the aged animals were almost completely disconnected from the other signaling modules in the aged

network, indicating a less diverse role of signaling in the aged animals. None of the TF-R pairs in the aged immune-tissue module were active in aged fibroblasts. Changes in cell communication can be further identified when the single cell cluster receptor-ligand information is overlaid on the communication score (**Extended Data Fig. 14**), and aging disruption of the immune-stromal communication can be more specifically identified (**Fig. 1f, bottom panel**). In particular, the stromal cluster vascular (Endo/Peri) and skeletal muscle cell (SMCs) communication with the T cells that were active in young mice during repair was severely diminished in aging mice, concordant with their reduced tissue repair[41]. T cell communication with the fibroblast population was also significantly diminished in the aged mice.

Next, we utilized a Bayesian non-negative matrix factorization (NMF) algorithm termed coordinate gene activity in pattern sets (CoGAPS) to capture additional gene sets representing cellular processes from the single cell dataset independent of changes in cell clusters[42] (**Fig. 1g**). NMF is an alternative method to infer expression patterns that can span multiple clusters, reflective of biological processes[43], with the Bayesian framework of CoGAPS having additional sparsity constraints ideal for scRNA-seq analysis. In the present dataset, CoGAPS found gene signatures of collagen production and assembly dominant in the muscle injury of aged animals (**Extended Data Fig. 15**), supporting the increased fibrosis observed histologically (**Extended Data Fig. 6**). More specifically, gene signatures associated with collagen markers, such as *Col1a1* and *Col1a2*, were enriched in fibroblasts from aged mice (**Fig. 1g, upper panel,** high expression cells in red). Furthermore, a set of genes related to collagen matrix assembly, including *Dcn*, *Fos*, and *Egr1*[44-46], was also more prominent in aged fibroblasts with ECM treatment showing the highest levels. When overlaid with the cell clusters, the gene patterns were closely associated with specific fibroblast clusters: generic collagen genes with Gen Fib and collagen matrix assembly gene sets with Mgp Fib (**Fig. 1g, upper panel circled with line**).

CoGAPS also highlighted gene profiles in the myeloid and macrophage cells that were dominant in young animals (**Fig. 1g, lower panel** and **Extended Data Fig. 16**). Genes associated with activated (*Lgals3*, *Gpx1*, *Vim*)[47,48] or regulatory (*Apoe*, *C1qb*, *Fcer1g*)[49,50] myeloid cells were all highly expressed in young animals compared to aged animals. While the treatment with ECM further increased the expression MHCII-associated genes (*Cd74*, *H2-Aa*, *H2-Eb1*) in both young and aged animals, their gene signatures were much more distinct within the young. When overlaid with cell clusters, we found an MHCII-associated gene pattern predominant in the Gen Myl cluster

(**Extended Data Fig. 9**), which increased with ECM treatment (**Extended Data Fig. 10**). The majority of additional gene patterns in myeloid and macrophage cells were also dominant in the young mice (**Extended Data Fig. 16**). This suggests that even though some cell clusters increased with ECM treatment in a similar manner between young and aged mice, they may have different gene signatures that impact functional outcomes. Furthermore, the loss of myeloid function in older animals may contribute to the impaired regeneration response to tissue injury and ECM biomaterials.

Altogether, the flow cytometry and single cell analysis demonstrate that key immune populations involved in muscle repair and a regenerative therapeutic response, such as eosinophils and CD4 T cells, decrease with aging. Furthermore, aging increases pro-inflammatory cells such as CD8 T cells and increases fibrosis signatures in response to regenerative treatments while at the same time decreasing immune activity features in myeloid and macrophages cells relevant for tissue repair including antigen presentation and immune cell mobilization.

Unique transcription factor activation identifies a type 3 immune profile in aging

To identify signaling components that may be responsible for reduced cell signaling and impaired wound healing with age from the single cell and Domino analysis, we compared the transcription factors and receptors active in the young and old networks (**Fig. 2a** and **Extended Data Fig. 11-13**). We identified several receptors common in both young and old signaling networks that correlated with activation of different TFs depending on age (**Extended Data Fig. 12-13**). These TFs are connected to IL4 and IL17 immune cytokine expression which negatively regulate each other to reinforce the differentiation pathways that were disrupted in the aging tissue. For example, we found transforming growth factor beta receptor 1 (*Tgfbr1*) in the immune-tissue module of young and aged animals correlated with *Batf* activation only in aged mice. *Batf* is one of the activator protein-1 (AP-1) proteins that controls Th17 differentiation[51], supporting the type 3 immune profile with aging. Additionally, a signal transduction adaptor *Tyrobp*, which was expressed in antigen processing modules in both age groups, correlated with *Batf3* activation, which regulates Th2 cell function while inhibiting the differentiation of regulatory T cells[52,53], only in old mice.

We then used String network to construct protein-protein interactions between the age-specific transcription factors discovered by Domino (**Fig. 2a, right panel** and **Extended Data Fig.**

17). The resulting network highlighted the aged animals-specific transcription factors, *Foxo3*, *Mef2c*, *Tcf7l2*, *Cebpa*, *Stat1*, and *Batf* as integral to the unique aging immune transcriptional network. To understand the biological significance of the age-specific TFs, we then performed gene set enrichment analysis using Enrichr[54,55], and enriched gene ontology (GO) terms to classify the biological processes in which they function (**Fig. 2b**). The young-specific TFs were associated with pathways involved with regulation of red blood cell differentiation or cytokinesis, and epithelial cell differentiation. On the other hand, aged animal-specific TFs were enriched for fat cell differentiation, Th17 differentiation and myeloid DC differentiation pathways. Signaling associated with Th17 differentiation is known to negatively regulate eosinophil recruitment and IL4 expression[56-58], suggesting that this immunological skewing in the TFs with aging may be responsible for the impaired Th2 response to the regenerative ECM biomaterial in the old animals.

To validate the computationally predicted type 3 immunological skewing in aged animals, we analyzed the baseline proximal inguinal lymph node (iLN). We first compared the gene expression profile of iLNs from naïve (no injury) young and aged mice using Nanostring analysis (**Fig. 2c** and **Extended Data Fig. 18-19**) and flow cytometry (**Fig. 2d** and **Extended Data Fig. 20**). Aged lymph nodes expressed lower levels of general T cell markers such as *Cd3e* and *Cd3d*, consistent with the known decrease in T cell numbers with aging. However, the expression of NF-κb/TNFα-, Fc receptor- or Th17-associated gene sets, all of which are potent inducers of Th17-mediated inflammation[59], increased in the aged lymph nodes (**Fig. 2c** and **Extended Data Fig. 18**). Pathway scoring further suggested that aging promoted T cell activation and skewing in Th17 differentiation or Th17-biology related gene expression (**Fig. 2c** and **Extended Data Fig. 19**). Flow cytometric analysis further supported a type 3-skewed immune environment in the aging lymph node with a significantly higher proportion of IL17A-producing CD4 and γδ T cells present in the aged iLN compared to the young (**Fig. 2d** and **Extended Data Fig. 20**). While both the Th1 ($IFN\gamma^+$ CD4) and Th17 ($IL17A^+$ CD4) cells increased with aging, the γδ T cells switched phenotype from type 1 ($IFN\gamma^+$) to type 3 ($IL17A^+$).

Aging CD4 T cells demonstrate a unique Th17 immune phenotype

To further evaluate the age-associated type 3 immune signatures, we evaluated whether aging CD4 T cells have a higher propensity for Th17 differentiation compared to young CD4 T cells (**Fig. 2e-g**). As expected, CD4 T cells isolated from the lymph nodes and spleen of aged animals exhibited

fewer naïve ($CD44^-CD62L^-$) but significantly higher percentages of effector ($CD44^+CD62L^-$) CD4 T cells compared to the young with the greatest difference found in cells isolated from the spleen (**Fig. 2e**). The effector T cells had notably higher percentages of RORγt expression, a lineage defining transcription factor of Th17 cells, particularly in cells isolated from the lymph node. To determine if the increased numbers of Th17 cells (**Fig. 2e**) was due to an increased propensity for differentiation, we isolated naïve CD4 T cells from the spleen of young and old animals, and cultured in Th17 skewing conditions *in vitro* (**Fig. 2f**). Naïve CD4 splenocytes from aged animals demonstrated significantly more effector cells and $ROR\gamma t^+$ Th17 cells when cultured in skewing conditions compared to young animals (**Fig. 2f, right panel**). In addition to increased skewing into $ROR\gamma t^+$ Th17 cells during *in vitro* culture, T cells from aged animals had a different secretome after skewing. Proteome analysis on the cells differentiated from naïve aging CD4 T cells showed significant upregulation in inflammatory cytokines, including IL12p40, a subunit for IL-23 that is required for Th17 differentiation, IL-6 family leukemia inhibitory factor (LIF), CCL5, CCL6, CCL22 and many others (**Fig. 2g**). This data suggests that naïve CD4 T cells from aging environment differentiate into a unique Th17 phenotype, and aging Th17 cells demonstrate a different secretory profile compared to young Th17 cells including more VEGF and CCL5, both of which play a direct role in angiogenesis.

Aging induces a local and systemic type 3 immune response to injury and biomaterial therapy

As the aged animals have higher baseline IL17 expression that increases significantly after injury and ECM treatment, we next analyzed in detail the source of IL17 (**Fig. 3**). Using young and aged IL17A-IRES-GFP-KI (IL17A-GFP) mice, we found γδ T cells, CD4 T cells, and innate lymphoid cells (ILC) all expressed IL17A after injury and increased in number after ECM treatment in both young and aged mice (**Extended Data Fig. 21**). The percentage of $IL17A^+$ γδ T cell, however, only significantly increased in aged animals with ECM treatment compared to injury alone and the percentage of $IL17A^+$ CD4 T cells increased only in aged animals with ECM treatment compared to no surgery (**Fig. 3b**). The percentage of ILCs expressing IL17A was similar among all groups except for naïve aged muscle tissue where there were significantly higher baseline levels, albeit in small cell numbers.

We then assessed the regional and systemic response to injury and ECM treatment in the lymph nodes and blood from young and aged mice (**Fig. 3c-g** and **Extended Data Fig. 22-24**). First, we observed visible differences in the size of the draining (inguinal) LNs with the young LNs appearing much larger before and after injury and increasing further in size with ECM treatment compared to the aged animals (**Fig. 3c**). Quantification of iLN volume using caliper measurements confirmed a significant increase in size in the young animals with ECM treatment. The LN size correlated with total cell numbers in iLN with injury and ECM treatment significantly increasing the number of $CD45^+$ cells in young animals, while only ECM treatment significant increased cell numbers in the aged animals albeit to a level significantly lower than young animals (**Extended Data Fig. 22**). In contrast to the lymph node, muscle tissue did not demonstrate significant differences in total $CD45^+$ cell number between young and aged animals after ECM treatment (**Extended Data Fig. 4**), suggesting that the lymph node highlights the age-associated immune and regenerative dysfunction that may be responsible for poor muscle regeneration with age.

Gene expression for canonical cytokines in the lymph node correlated with the immune profiles found in the muscle tissue. ECM treatment significantly increased *Il4* expression in young iLNs only (**Fig. 3d**) and there were minimal changes in *Ifnγ* expression. Strikingly, both *Il17a* and *Il17f* expression significantly increased only in aged animals after injury and ECM treatment. We further analyzed the expression of genes that relate to Th17 skewing, as defined by String network analysis; *Mmp3*, *Mmp9*, *Cxcl1*, *Ccl20*, and *Cxcl5*[60]. Expression of these genes occurred at low levels in all conditions in naïve young and aged animals but significantly increased only after injury and ECM treatment in aged mice (**Fig. 3e**), suggesting that injury further triggered a type 3 immune response beyond the baseline in an aging tissue environment. Multiparametric flow cytometry analysis of the cells from the iLN further confirmed the trend with increasing numbers and percentages of $IL17A^+$ γδ and CD4 T cells after ECM treatment only in aged mice (**Fig. 3f** and **Extended Data Fig. 23**). In addition, B cells also exhibited age-specific changes after injury and ECM treatment (**Extended Data Fig. 22**). Similar to the increased number of B cells in aging muscle tissue (**Extended Data Fig. 4**), iLN from old animals had significantly higher percentages of B cells after injury and treatment, further skewing T to B cell ratio with age.

To further assess the systemic immune changes with aging, we analyzed cytokines in serum using proteome profiler (**Fig. 3g** and **Extended Data Fig. 24**). In addition to increased IL17 in the

serum of aged mice, there was also increased level of the B cell chemoattractant factor CXCL13, suggesting that the increased B cell signatures in aged muscle and lymph nodes also extended systemically. CXCL13 also significantly increased in blood after injury in old mice (**Extended Data Fig. 24**), further supporting that injury promotes a B cell response solely in old animals where the overall number of T cells and naïve T cells is significantly reduced. Additionally, IL1A, a potent inducer of IL17 from T cells[61], and CXCL1, one of IL17-induced chemokines, also increased in serum from the aged mice. IL23, a protein that can expand Th17 cells[62], increased in response to injury only in old mice. Collectively, these data show that injury and ECM treatment in aged animals triggered a local and systemic type 3-mediated immune response that may be responsible for the decreased regenerative and therapeutic response with aging.

Inhibition of IL17 rejuvenates type 2 response after muscle injury in aged animals

Since IL17 is associated with fibrosis[63,64] and negatively regulates IL4 that is needed for tissue repair, we investigated if IL17 neutralizing antibodies (αIL17) could restore IL4 expression and tissue repair that is lost with aging. We first evaluated the dose and timing for delivery (**Extended Data Fig. 25**). A minimum of three injections was required to reduce inflammatory markers in the tissue after injury in aged mice. However, initiating αIL17 injections at the time of injury stunted infiltration of immune ($CD45^+$) cells including $IL4^+$ cells that are critical for tissue repair, suggesting the importance of acute IL17 during wound healing to attract the immune effectors and initiate tissue regeneration (**Extended Data Fig. 25b**). We then tested initiation of αIL17 injections one week after injury to allow immune infiltration before treatment (**Fig. 4a**). Using aged $Il4^{tm1Lky}$ mice (4Get), which have a fluorescent reporter for IL4 expression, we found that both αIL17A and αIL17F treatment one week after injury significantly increased the number of $IL4^+$ eosinophils and CD4 T cells three weeks after injury.

Combination therapy of pro-regenerative ECM and αIL17 rejuvenates muscle repair in aged mice

Since αIL17 treatment alone restored IL4 expression after injury in aged animals, we tested a combination therapy approach with pro-regenerative ECM and αIL17 (**Fig. 4b**). Muscle wounds in aged animals received ECM treatment at the time of surgery and local αIL17 one week after injury. Six weeks after injury in aged 4Get mice, the antibody treatment after ECM implantation

increased $CD45^+$ cell numbers (**Extended Data Fig. 26**), however, only the αIL17A treated animals had a significantly higher number and percentage of $IL4^+CD45^+$ immune cells, and number of $IL4^+CD4^+$ T cells compared to the αIL17F or ECM only groups, albeit in small numbers at this later time point. Three weeks after combination therapy, we observed a significant decrease in γδ T cell numbers, a major source of IL17, in mice treated with αIL17A or αIL17F using multi-spectral flow cytometry (**Extended Data Fig. 27**).

We then explored the therapeutic response to ECM-αIL17 combination in the muscle wound and tissue repair. Six weeks after injury, muscle tissue from aged C57BL/6J mice treated with ECM and αIL17A expressed significantly lower levels of numerous fibrosis- or adipose-associated genes that CoGAPS analysis identified as increasing in aged animals (**Fig. 4c, top left panel**). Specifically, collagen type III a1 (*Col3a1*) and collagen type V a1 (*Col5a1*) decreased significantly only with ECM-αIL17A combination treatment. Additionally, adipose-associated genes, such as *Pparγ*, *Fabp4*, and *Adipoq* all dramatically decreased with αIL17A treatment. Other fibrosis-related genes, such as *Fap* and *Pdgfa*[65], decreased with αIL17A or αIL17A/αIL17F (**Extended Data Fig. 28**). Expression of the inflammatory gene *Mmp13* significantly decreased with any combination of αIL17 treatments, however, RAR-related orphan receptor type c (*Rorc*), which is critical in the differentiation of Th17[66], was only downregulated with a combination of αIL17A/αIL17F treatment. Differences in gene expression profile between the αIL17A and αIL17F-treated groups suggest that there may be a distinction between IL17a and IL17f signaling pathways.

Histological evaluation of the muscle defect in aged animals treated with combination therapy supported the immunological and gene expression results with increased repair and reduced fibrosis depending on the form of IL17 neutralization (**Fig. 4c** and **Extended Data Fig. 29**). Aged mice treated with ECM alone demonstrated collagen deposition and fibrosis that decreased with αIL17A or combination αIL17A/αIL17F treatment as visualized by Masson's trichrome. Adipose deposition in the repaired tissue also decreased with ECM-αIL17A combination treatment as visualized in the histology, supporting the gene expression results. Additionally, a combination treatment induced nuclear repositioning from the periphery to the center of muscle cells (**Fig. 4d**), a characteristic of repairing muscle tissue that did not occur in animals treated with injury or ECM alone. Nuclear positioning is critical in muscle fiber function, and it was shown that myofibers that are regenerated several weeks after muscle damage can be

characterized by centrally localized nuclei[67,68]. Quantification of muscle cells with centrally-located nuclei demonstrated that ECM-αIL17A combination treatment significantly increased the percentage of regenerating muscle fibers compared to the injury or ECM alone groups (**Fig. 4d, right panel**). Altogether, we demonstrate that aging significantly alters the immune and stromal response to muscle injury and therapeutic biomaterials in the local tissue, regional lymph nodes and systemically in blood. These altered responses, characterized by increased IL17, reduced IL4 and excess fibrosis and adipogenesis, can be mitigated with a combination therapy of a pro-regenerative ECM material and an IL17 antibody to promote the repair capacity in aging tissue.

Discussion

In this work, we uncovered age-related changes associated with type 3 (IL17) immunity that are present in secondary lymphoid organs, that is further exacerbated after muscle injury and treatment with a regenerative ECM biomaterial. Repaired tissue in the aged animals is characterized by excessive fibrosis and adipose tissue with treatment. Single cell analysis revealed excessive collagen activity and abnormalities in myeloid and antigen presentation in the aged animals. Cell communication highlighted diminished immune-stromal cell interactions with aging, particularly between aged T cells, which had an altered secretome, and vascular-related clusters (endo/peri) and muscle cells. Combination therapy of the ECM scaffold with an IL17 neutralizing antibody in the aged animals restored, in part, the pro-regenerative immune response and tissue repair while reducing fibrosis and excess adipose.

Tissue injury mobilizes the immune system and uncovers new age-associated dysfunctions that may not be otherwise apparent. Aging is associated with numerous chronic diseases and increased incidence of cancer[69]. Healthy aging though, even without overt disease, results in longer recovery times from tissue injury. Changes in cellular composition with aging may be in part responsible for reduced healing capacity including decreased endogenous stem cell numbers and activity, in addition to reduced fibroblast heterogeneity[8,9]. However, the pivotal role of the immune system in the response to tissue injury and directing tissue repair is critical to consider as there are many age-related changes in the immune system. Even the epigenetic changes that have been implicated in age-associated repair dysfunction[70] may extend to the aging immune response to tissue damage as we observed a different secretome of aged Th17 skewed cells cultured in similar conditions to young T cells that is likely due to epigenetic changes. As regenerative medicine

strategies are moving to target the immune system, understanding these age-associated immune changes will be critical to develop regenerative immunotherapies that are relevant to the older patient populations that are more likely to suffer from delayed or inadequate tissue repair. Finally, as biological age does not always correlate with chronological age, relevant diagnostics and personalized therapeutic approaches may be needed.

While multiple regenerative medicine therapies are available, we chose ECM biomaterials to evaluate in an aging environment because of their clinical use[16]. Few regenerative medicine therapies have reached standard clinical practice and now even the mechanism of long-studied stem cell therapies is being reconsidered, as non-viable cells appear to promote similar therapeutic responses as viable cells[71]. ECM biomaterials derived from allograft and porcine sources are approved for wound healing and reconstructive surgery applications, orthopedic, and ophthalmologic indications[16,72,73]. ECM materials contain a complex mixture of proteins, proteoglycans, and even matrix-bound vesicles that likely all contribute to damage signals and other as yet determined factors that mobilize multiple immune and stromal cell types to promote tissue repair. It is likely that other regenerative medicine approaches, cellular, growth factors or small molecules, will exhibit similar reduced efficacy with aging that we found using ECM.

Aged animals exhibited a baseline inflammatory state with more $CD8^+$ T cells and Th17 cells, the latter being most predominant in the lymph nodes. In the muscle tissue, however, IL17 expression was only observed after injury and ECM treatment, which induced the most significant increases in IL17. While *Il17a* and *f* were observed in the lymph node, only *Il17f* gene expression was found in the muscle tissue. Injury in the older animals uncovered many age-related signatures associated with IL17 and its signaling, and this was further exacerbated with ECM implantation. The cytokine IL17 is a component of the host defense against extracellular pathogens[56,74], but is also associated with fibrosis and fibrotic disease[63,64], suggesting a common mechanism of "walling off" uncontrolled pathogens and maintaining barrier surfaces and microbiome balance. While IL17 is important for the recruitment of effector immune cells for wound repair and host defense, its chronic state with aging can further induce carcinogenesis, fibrosis, and inappropriate immune responses. Age-associated commensal dysbiosis may contribute to the excess IL17 in addition to senescence-induced immunomodulation that promotes IL17[75]. As mice are reared in a controlled lab environment, the increased aged-associated IL17 related to gut dysbiosis may be even greater and more variable in people that have more diverse environment exposure, diet, and etc.

Cell communication analysis by Domino uncovered active immune-stromal module interactions in young animals that were impaired and limited in an aging environment. Young mice demonstrated immune-stromal communication associated with vascular development and muscle cell activity, both of which are well recognized for their roles in tissue repair. Interestingly, the aged Th17-skewed cells secreted more VEGF *in vitro* compared to the young T cells, suggesting a possible epigenetic memory associated with vascular insufficiency. In addition to VEGF, the aged Th17 cells also secreted increased levels of LIF, a component of the Stat3 and Wnt signaling pathway involved in vascular development. Vascular insufficiency and impaired VEGF signaling is a hallmark of aging, particularly in the microvasculature which is a necessary component of tissue repair regeneration[76]. We also previously showed that inflammatory (Th17)-induced senescent cells produce a senescence-associated secretory phenotype that upregulated Wnt signaling genes, such as Wnt5b and Wnt11, further implicating Wnt signaling in age-related repair dysfunction.

In summary, the immune system represents an exciting new therapeutic target for regenerative medicine. However, the complexity of the immune system in people and variability related to intrinsic genetic, sex differences, exposure history and environmental factors that only increases with age must be considered in therapeutic design. Combination therapies, a standard approach in cancer treatment, should be extended to regenerative medicine where complex interactions between the immune system, stem cells, and the vascular system contribute to repair outcomes.

Acknowledgements

This work was funded in part by the National Institutes of Health (NIH) Pioneer Award DP1AR076959 (J.H.E.), Bloomberg~Kimmel Institute, Morton Goldberg Professorship (J.H.E.), the Department of Defense, R01EB028796 (J.H.E.), R01AG063801(J.H.E.). A.R. and D.R.M. were funded through NSF GRFP DGE-1746891. We thank F. Housseau for providing the IL17A-GFP mice. Schematic illustrations created with BioRender.com.

Author contributions

J.H., and J.H.E. conceptualized the study, drafted, and edited the figures and manuscript. J.H., J.H.E., and D.M.P. contributed to experimental design and interpretation of the results. J.H.

performed animal surgery model and analyzed experimental results (flow cytometry, qRT-PCR, proteome profiler, histology, and analysis). C.C. wrote software and assisted in single cell RNA sequencing analysis and computational methodology. A.R., J.C.M., and D.R.M. assisted with animal breeding and spectral flow cytometry analysis. H.H.N. contributed to conducting histological evaluation. A.N.P, B.Y., N.R., E.G.G., and E.M.M. assisted with *in vitro* T cell culture or subsequent genomic profile assessment. E.J.F. advised in the bioinformatics analysis. F.H., S.G., and A.J.T. assisted with generalized gene expression interpretation and flow cytometry results.

Competing interests

JHE holds equity in Unity Biotechnology and Aegeria Soft Tissue and is an advisor for Tessera Therapeutics, HapInScience, and Font Bio. DMP is consultant at Aduro Biotech, Amgen, Astra Zeneca, Bayer, Compugen, DNAtrix, Dynavax Technologies Corporation, Ervaxx, FLX Bio, Immunomic, Janssen, Merck, and Rock Springs Capital. DMP holds equity in Aduro Biotech, DNAtrix, Ervaxx, Five Prime therapeutics, Immunomic, Potenza, Trieza Therapeutics. DMP is a member of the scientific advisory board for Bristol Myers Squibb, Camden Nexus II, Five Prime Therapeutics, and WindMil. DMP is a member of board of directors in Dracen Pharmaceuticals. CC is the founder and owner of C M Cherry Consulting, LLC. EJF is a member of the scientific advisory board for Viosera Therapeutics.

References

1. Kirkwood, T.B. Understanding the odd science of aging. *Cell* **120**, 437-447 (2005).
2. Pisco, A.O., *et al.* A single cell transcriptomic atlas characterizes aging tissues in the mouse. *BioRxiv*, 661728 (2019).
3. van Deursen, J.M. The role of senescent cells in ageing. *Nature* **509**, 439-446 (2014).
4. Du Noüy, P.L. Cicatrization of wounds: III. The relation between the age of the patient, the area of the wound, and the index of cicatrization. *J Exp Med* **24**, 461-470 (1916).
5. Gosain, A. & DiPietro, L.A. Aging and wound healing. *World J Surg* **28**, 321-326 (2004).
6. Gould, L., *et al.* Chronic wound repair and healing in older adults: current status and future research. *J Am Geriatr Soc* **63**, 427-438 (2015).
7. Emery, C.F., Kiecolt-Glaser, J.K., Glaser, R., Malarkey, W.B. & Frid, D.J. Exercise accelerates wound healing among healthy older adults: a preliminary investigation. *J Gerontol A Biol Sci Med Sci* **60**, 1432-1436 (2005).
8. Mahmoudi, S., *et al.* Heterogeneity in old fibroblasts is linked to variability in reprogramming and wound healing. *Nature* **574**, 553-558 (2019).
9. Cosgrove, B.D., *et al.* Rejuvenation of the muscle stem cell population restores strength to injured aged muscles. *Nat Med* **20**, 255-264 (2014).
10. Pennington, K.L. & DeAngelis, M.M. Epigenetic Mechanisms of the Aging Human Retina. *J Exp Neurosci* **9**, 51-79 (2015).
11. Howard, D., Buttery, L.D., Shakesheff, K.M. & Roberts, S.J. Tissue engineering: strategies, stem cells and scaffolds. *J Anat* **213**, 66-72 (2008).
12. Franceschi, C., Garagnani, P., Parini, P., Giuliani, C. & Santoro, A. Inflammaging: a new immune-metabolic viewpoint for age-related diseases. *Nat Rev Endocrinol* **14**, 576-590 (2018).
13. Castle, S.C. Clinical relevance of age-related immune dysfunction. *Clin Infect Dis* **31**, 578-585 (2000).
14. Nikolich-Zugich, J. Ageing and life-long maintenance of T-cell subsets in the face of latent persistent infections. *Nat Rev Immunol* **8**, 512-522 (2008).
15. Pang, W.W., *et al.* Human bone marrow hematopoietic stem cells are increased in frequency and myeloid-biased with age. *Proc Natl Acad Sci U S A* **108**, 20012-20017 (2011).
16. Badylak, S.F., Freytes, D.O. & Gilbert, T.W. Extracellular matrix as a biological scaffold material: Structure and function. *Acta Biomater* **5**, 1-13 (2009).
17. Brown, B.N., *et al.* Macrophage phenotype as a predictor of constructive remodeling following the implantation of biologically derived surgical mesh materials. *Acta Biomater* **8**, 978-987 (2012).
18. Mase, V.J., Jr., *et al.* Clinical application of an acellular biologic scaffold for surgical repair of a large, traumatic quadriceps femoris muscle defect. *Orthopedics* **33**, 511 (2010).
19. Lee, K., Silva, E.A. & Mooney, D.J. Growth factor delivery-based tissue engineering: general approaches and a review of recent developments. *J R Soc Interface* **8**, 153-170 (2011).
20. Teodori, L., *et al.* Native extracellular matrix: a new scaffolding platform for repair of damaged muscle. *Front Physiol* **5**, 218 (2014).
21. Wang, Z., *et al.* Novel biomaterial strategies for controlled growth factor delivery for biomedical applications. *NPG Asia Mater* **9**, e435-e435 (2017).

22. Mosala Nezhad, Z., *et al.* Small intestinal submucosa extracellular matrix (CorMatrix(R)) in cardiovascular surgery: a systematic review. *Interact Cardiovasc Thorac Surg* **22**, 839-850 (2016).
23. Gieseck III, R.L., Wilson, M.S. & Wynn, T.A. Type 2 immunity in tissue repair and fibrosis. *Nat Rev Immunol* **18**, 62 (2018).
24. Heredia, J.E., *et al.* Type 2 innate signals stimulate fibro/adipogenic progenitors to facilitate muscle regeneration. *Cell* **153**, 376-388 (2013).
25. Sadtler, K., *et al.* Developing a pro-regenerative biomaterial scaffold microenvironment requires T helper 2 cells. *Science* **352**, 366-370 (2016).
26. Janson, D.G., Saintigny, G., van Adrichem, A., Mahe, C. & El Ghalbzouri, A. Different gene expression patterns in human papillary and reticular fibroblasts. *J Invest Dermatol* **132**, 2565-2572 (2012).
27. Korosec, A., *et al.* Lineage Identity and Location within the Dermis Determine the Function of Papillary and Reticular Fibroblasts in Human Skin. *J Invest Dermatol* **139**, 342-351 (2019).
28. Haydont, V., Neiveyans, V., Fortunel, N.O. & Asselineau, D. Transcriptome profiling of human papillary and reticular fibroblasts from adult interfollicular dermis pinpoints the 'tissue skeleton' gene network as a component of skin chrono-ageing. *Mech Ageing Dev* **179**, 60-77 (2019).
29. Sole-Boldo, L., *et al.* Single-cell transcriptomes of the human skin reveal age-related loss of fibroblast priming. *Commun Biol* **3**, 188 (2020).
30. Singhmar, P., *et al.* The fibroblast-derived protein PI16 controls neuropathic pain. *Proc Natl Acad Sci U S A* **117**, 5463-5471 (2020).
31. Calcagno, D.M., *et al.* SiglecF(HI) Marks Late-Stage Neutrophils of the Infarcted Heart: A Single-Cell Transcriptomic Analysis of Neutrophil Diversification. *J Am Heart Assoc* **10**, e019019 (2021).
32. Xie, X., *et al.* Single-cell transcriptome profiling reveals neutrophil heterogeneity in homeostasis and infection. *Nat Immunol* **21**, 1119-1133 (2020).
33. Agier, J., Efenberger, M. & Brzezinska-Blaszczyk, E. Cathelicidin impact on inflammatory cells. *Cent Eur J Immunol* **40**, 225-235 (2015).
34. Zhang, X.J., *et al.* Distinctive structural hallmarks and biological activities of the multiple cathelicidin antimicrobial peptides in a primitive teleost fish. *J Immunol* **194**, 4974-4987 (2015).
35. Kalantari, P., Bunnell, S.C. & Stadecker, M.J. The C-type Lectin Receptor-Driven, Th17 Cell-Mediated Severe Pathology in Schistosomiasis: Not All Immune Responses to Helminth Parasites Are Th2 Dominated. *Front Immunol* **10**, 26 (2019).
36. Kalantari, P., *et al.* CD209a Synergizes with Dectin-2 and Mincle to Drive Severe Th17 Cell-Mediated Schistosome Egg-Induced Immunopathology. *Cell Rep* **22**, 1288-1300 (2018).
37. Ponichtera, H.E., *et al.* CD209a expression on dendritic cells is critical for the development of pathogenic Th17 cell responses in murine schistosomiasis. *J Immunol* **192**, 4655-4665 (2014).
38. Wang, J., *et al.* A Positive Feedback Loop Between Th17 Cells and Dendritic Cells in Patients with Endplate Inflammation. *Immunol Invest* **48**, 39-51 (2019).
39. Aibar, S., *et al.* SCENIC: single-cell regulatory network inference and clustering. *Nat Methods* **14**, 1083-1086 (2017).

40. Cherry, C., *et al.* Intercellular signaling dynamics from a single cell atlas of the biomaterials response. *bioRxiv* (2020).
41. Yin, H., Price, F. & Rudnicki, M.A. Satellite cells and the muscle stem cell niche. *Physiol Rev* **93**, 23-67 (2013).
42. Stein-O'Brien, G.L., *et al.* Decomposing Cell Identity for Transfer Learning across Cellular Measurements, Platforms, Tissues, and Species. *Cell Syst* **8**, 395-411 e398 (2019).
43. Stein-O'Brien, G.L., *et al.* Enter the Matrix: Factorization Uncovers Knowledge from Omics. *Trends Genet* **34**, 790-805 (2018).
44. Zhang, W., *et al.* Decorin is a pivotal effector in the extracellular matrix and tumour microenvironment. *Oncotarget* **9**, 5480-5491 (2018).
45. Havis, E. & Duprez, D. EGR1 Transcription Factor is a Multifaceted Regulator of Matrix Production in Tendons and Other Connective Tissues. *Int J Mol Sci* **21**(2020).
46. Rosenfeldt, H., Lee, D.J. & Grinnell, F. Increased c-fos mRNA expression by human fibroblasts contracting stressed collagen matrices. *Mol Cell Biol* **18**, 2659-2667 (1998).
47. Park, D.D., *et al.* Resident and elicited murine macrophages differ in expression of their glycomes and glycan-binding proteins. *Cell Chem Biol* **28**, 567-582. e564 (2021).
48. Mor-Vaknin, N., Punturieri, A., Sitwala, K. & Markovitz, D.M. Vimentin is secreted by activated macrophages. *Nat Cell Biol* **5**, 59-63 (2003).
49. Poon, C.C., *et al.* Differential microglia and macrophage profiles in human IDH-mutant and-wild type glioblastoma. *Oncotarget* **10**, 3129 (2019).
50. Gu, Z., Chhabra, A., Alard, P., Warner, D. & Kosiewicz, M. FcγRI is required for TGFβ2-treated macrophage-induced tolerance. *Immunobiology* **218**, 1200-1206 (2013).
51. Ciofani, M., *et al.* A validated regulatory network for Th17 cell specification. *Cell* **151**, 289-303 (2012).
52. Kuwahara, M., *et al.* Bach2-Batf interactions control Th2-type immune response by regulating the IL-4 amplification loop. *Nat Commun* **7**, 12596 (2016).
53. Lee, W., Kim, H.S., Hwang, S.S. & Lee, G.R. The transcription factor Batf3 inhibits the differentiation of regulatory T cells in the periphery. *Exp Mol Med* **49**, e393 (2017).
54. Chen, E.Y., *et al.* Enrichr: interactive and collaborative HTML5 gene list enrichment analysis tool. *BMC Bioinformatics* **14**, 128 (2013).
55. Kuleshov, M.V., *et al.* Enrichr: a comprehensive gene set enrichment analysis web server 2016 update. *Nucleic Acids Res* **44**, W90-97 (2016).
56. Schmidt-Weber, C.B., Akdis, M. & Akdis, C.A. TH17 cells in the big picture of immunology. *J Allergy Clin Immunol* **120**, 247-254 (2007).
57. Lin, P.Y., Jen, H.Y., Chiang, B.L., Sheu, F. & Chuang, Y.H. Interleukin-21 suppresses the differentiation and functions of T helper 2 cells. *Immunology* **144**, 668-676 (2015).
58. Ohnmacht, C., *et al.* The microbiota regulates type 2 immunity through RORγt+ T cells. *Science* **349**, 989-993 (2015).
59. Liu, T., Zhang, L., Joo, D. & Sun, S.-C. NF-κB signaling in inflammation. *Signal Transduct Target Ther* **2**, 1-9 (2017).
60. Xu, S. & Cao, X. Interleukin-17 and its expanding biological functions. *Cell Mol Immunol* **7**, 164-174 (2010).
61. Sutton, C., Brereton, C., Keogh, B., Mills, K.H. & Lavelle, E.C. A crucial role for interleukin (IL)-1 in the induction of IL-17–producing T cells that mediate autoimmune encephalomyelitis. *J Exp Med* **203**, 1685-1691 (2006).

62. Bunte, K. & Beikler, T. Th17 Cells and the IL-23/IL-17 Axis in the Pathogenesis of Periodontitis and Immune-Mediated Inflammatory Diseases. *Int J Mol Sci* **20**, 3394 (2019).
63. Fabre, T., *et al.* Type 3 cytokines IL-17A and IL-22 drive TGF-beta-dependent liver fibrosis. *Sci Immunol* **3**(2018).
64. Tesmer, L.A., Lundy, S.K., Sarkar, S. & Fox, D.A. Th17 cells in human disease. *Immunol Rev* **223**, 87-113 (2008).
65. Malecova, B., *et al.* Dynamics of cellular states of fibro-adipogenic progenitors during myogenesis and muscular dystrophy. *Nat Commun* **9**, 3670 (2018).
66. Yang, X.O., *et al.* T helper 17 lineage differentiation is programmed by orphan nuclear receptors RORα and RORγ. *Immunity* **28**, 29-39 (2008).
67. Folker, E.S. & Baylies, M.K. Nuclear positioning in muscle development and disease. *Front Physiol* **4**, 363 (2013).
68. Cadot, B., Gache, V. & Gomes, E.R. Moving and positioning the nucleus in skeletal muscle–one step at a time. *Nucleus* **6**, 373-381 (2015).
69. Prasad, S., Sung, B. & Aggarwal, B.B. Age-associated chronic diseases require age-old medicine: role of chronic inflammation. *Prev Med* **54 Suppl**, S29-37 (2012).
70. Pal, S. & Tyler, J.K. Epigenetics and aging. *Sci Adv* **2**, e1600584 (2016).
71. Wagoner, Z.W. & Zhao, W. Therapeutic implications of transplanted-cell death. *Nat Biomed Eng* **5**, 379-384 (2021).
72. Liu, L., *et al.* Evaluation of the biocompatibility and mechanical properties of xenogeneic (porcine) extracellular matrix (ECM) scaffold for pelvic reconstruction. *Int Urogynecol J* **22**, 221-227 (2011).
73. Chow, D.W. & Westermeyer, H.D. Retrospective evaluation of corneal reconstruction using AC ell Vet™ alone in dogs and cats: 82 cases. *Vet Ophthalmol* **19**, 357-366 (2016).
74. Martinez, G.J., Nurieva, R.I., Yang, X.O. & Dong, C. Regulation and function of proinflammatory TH17 cells. *Ann N Y Acad Sci* **1143**, 188-211 (2008).
75. Faust, H.J., *et al.* IL-17 and immunologically induced senescence regulate response to injury in osteoarthritis. *J Clin Invest* **130**, 5493-5507 (2020).
76. Grunewald, M., *et al.* Counteracting age-related VEGF signaling insufficiency promotes healthy aging and extends life span. *Science* **373**(2021).

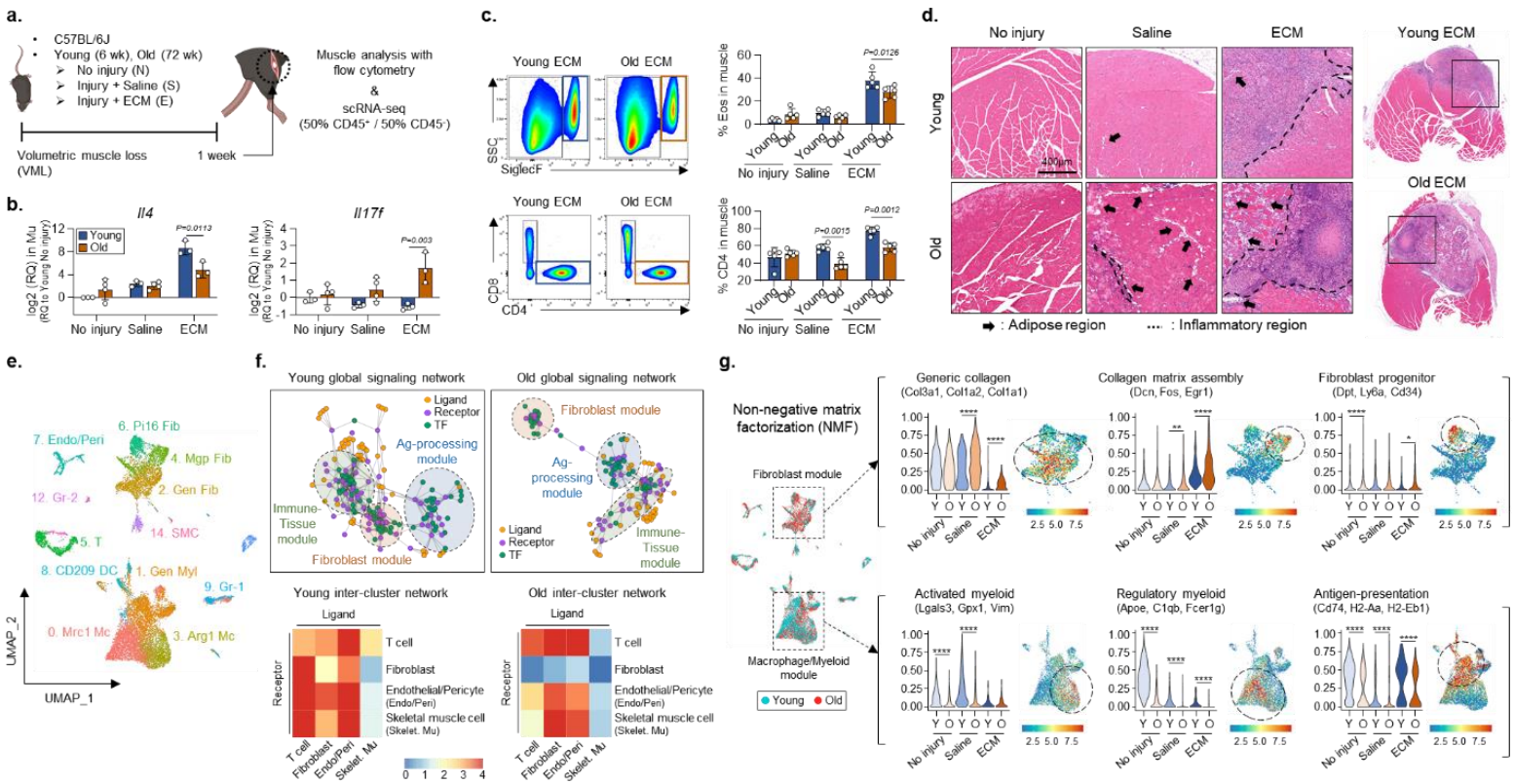

Figure 1. Aging alters immune-stromal response to regenerative ECM biomaterials and impairs immune-stromal communication in muscle. a, Schematic illustration of experimental design including no injury control (N), volumetric muscle loss injury treated with saline (S) and VML treated with ECM (E) in young (6 wk) and old (72 wk). **b**, Quantification of Th2 or Th17-related genes in muscle 1 week after injury or ECM treatment (n=3 young; n=3-4 old). **c**, Quantification of immune cells from spectral flow cytometry with significant population changes between young and old mice with muscle injury and treatment (n=5). Eosinophils are presented as % of $CD11b^+$, NKTs % of $CD3^+\gamma\delta^-$, and CD4 or CD8 % of $CD3^+\gamma\delta^-NK^-$. **d**, Transverse section of the quadricep muscle 1 week after injury or ECM stained with H&E. The black arrow indicates the ectopic adipogenesis region, and the dotted line demonstrates immune cell infiltrated area. **e**, UMAP overview of cell clusters identified using scRNA-seq data set on muscle from young and aged animals with injury or treatment (3 mice pooled for each condition). **f**, Age-specific global signaling network (top) and heatmap of predicted cluster-cluster signaling for selected clusters determined by Domino (bottom). The values shown are the summed z-scored expression values for ligands (in the ligand-cluster) targeting receptors predicted to be activated in the receptor-cluster. Higher values indicate increased expression of ligands predicted to be active for a given receptor cluster. **g**, NMF-CoGAPS analysis of fibroblast populations (top) and myeloid/macrophage populations (bottom). Region of cells expressing high levels of the gene sets are circled. Two-way ANOVA with Tukey's multiple comparisons test in (**b-c**). *p* values in NMF-CoGAPS were determined using Mann-Whitney U test and adjusted with false discovery rate correction for multiple testing in (**g**). **p*<0.05, ***p*<0.01, and *****p*<0.0001. For all bar graphs, data are mean ± s.d.

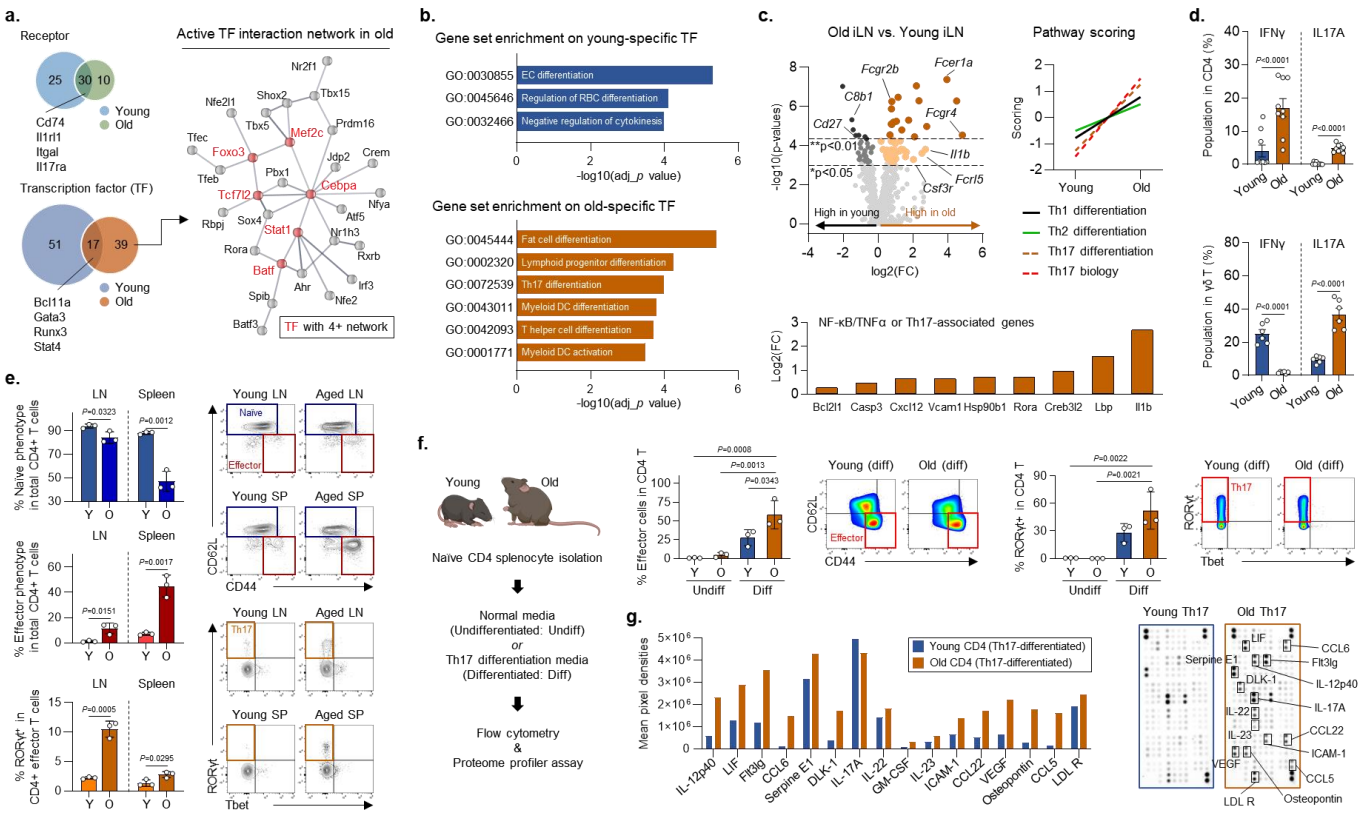

Figure 2. Aging induces a Th17-associated transcription network and aged CD4 T cells demonstrate increased Th17 skewing and a unique secretome. a, Venn diagram illustrating shared or age-specific receptors and TFs (left), and protein-protein interaction network for the TFs specific to aged animals using STRING network (right). **b**, Gene set enrichment analysis using Enrichr of age-specific TFs in muscle. Adjusted *p* value (log 10) of significant GO terms are shown. **c**, Volcano plot of genes expressed in aged lymph node normalized to those in young lymph node (top left). Gene scoring for helper T cell pathways (top right) or differentially expressed genes for NF-κb/TNFα or Th17-associated pathways (bottom) based on Nanostring analysis (n=6). **d**, Multiparametric flow cytometry quantification of IFNγ$^+$ or IL17A$^+$ CD4 or γδ T cells in the lymph nodes from young or aged animals without injury or treatment (n=9 CD4 T; n=6 γδ T). **e**, Quantification (left) and representative plots (right) of flow cytometry analysis on CD4 T cells isolated from lymph nodes or spleens of young and old animals. Naïve phenotype (CD4$^+$CD44$^-$CD62L$^-$), effector phenotype (CD4$^+$CD44$^+$CD62L$^-$) and Th17 cells (CD4$^+$CD44$^+$CD62L$^-$RORγt$^+$) are shown (n=3). **f**, Schematic illustration of naïve T cell isolation and Th17 differentiation *in vitro* (left) and quantification of flow cytometry analysis on the undifferentiated and differentiated CD4 T cells (right; n=3). **g**, Quantification (left) and representative images (right) of the proteome profiler performed on cell culture supernatant from Th17-differentiated CD4 T cells from young and old mice (3 samples pooled for each condition). Protein molecules with significant differences in pixel densities compared to young animals are labeled and quantified using iBright Analysis Software. Unpaired two-tailed t-test (**d-e**). Two-way ANOVA with Tukey's multiple comparisons test (**f**). For all bar graphs, data are mean ± s.e.m (**d**) or s.d. (**e-f**).

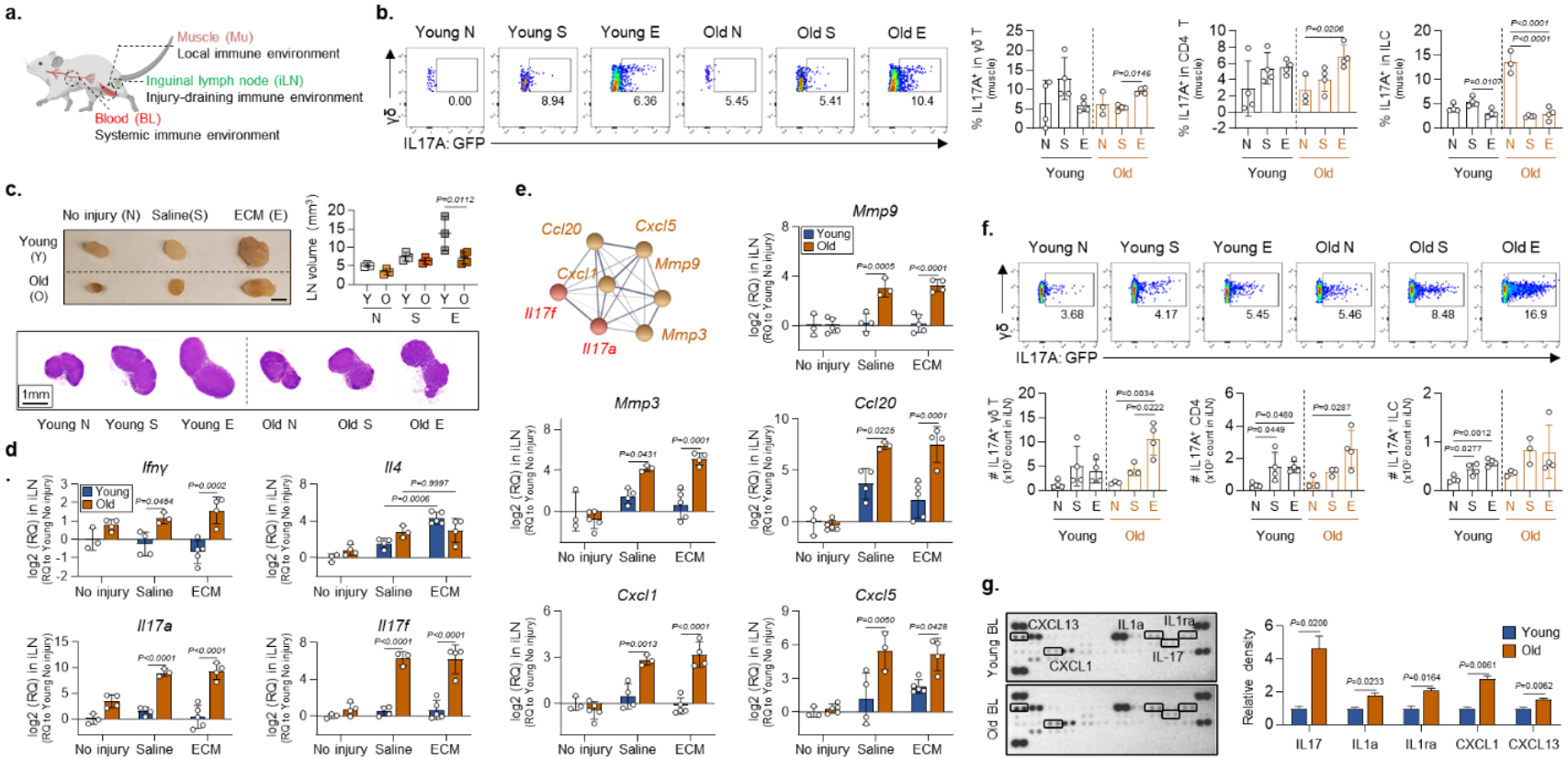

Figure 3. Injury and ECM treatment in aged animals promote local and systemic IL17-associated immune response that inhibits tissue repair. a, Schematic illustration of various immune environments that are affected by injury. **b**, Representative images of flow cytometry comparing IL17A$^+$ γδ T cells between young and aged animals (left) and the quantification of IL17 producing cell subtypes in muscle 1 week after injury or ECM treatment (n=3-4); γδ T cell, CD4 T cell, and innate lymphoid cell (ILC). **c-f**, in lymph node 1 week after injury or ECM treatment. **c**, Representative images of the lymph nodes (top left) and the quantification of their size (top right). Scale bar, 2mm. Transverse section of the lymph nodes is stained with H&E (bottom). **d**, Quantification of T helper cell cytokine-related genes in lymph node (n=3-5 young; n=3-4 old). **e**, Quantification of Th17-associated genes in the lymph nodes (n=3-5). Protein-protein interaction demonstrating their association with IL17A or IL17F are shown using STRING network (top left). **f**, Representative images of flow cytometry data comparing IL17A$^+$ γδ T cells between young and aged animals (top) and the quantification of IL17 producing cell subtypes in the lymph node (n=3-4). **g**, Representative images (left) and quantitative analysis (right) of the proteome profiler performed on blood serum from young and aged mice without the treatments (3 mice pooled for each condition). Protein molecules with significant differences in pixel densities compared to young animals are labeled and quantified using imageJ. Two-way ANOVA with Tukey's multiple comparisons test (**c-e**), one-way ANOVA with Tukey's multiple comparisons test (**b**, **f**), unpaired two-tailed t-test (**g**). For all bar graphs, data are mean ± s.d.

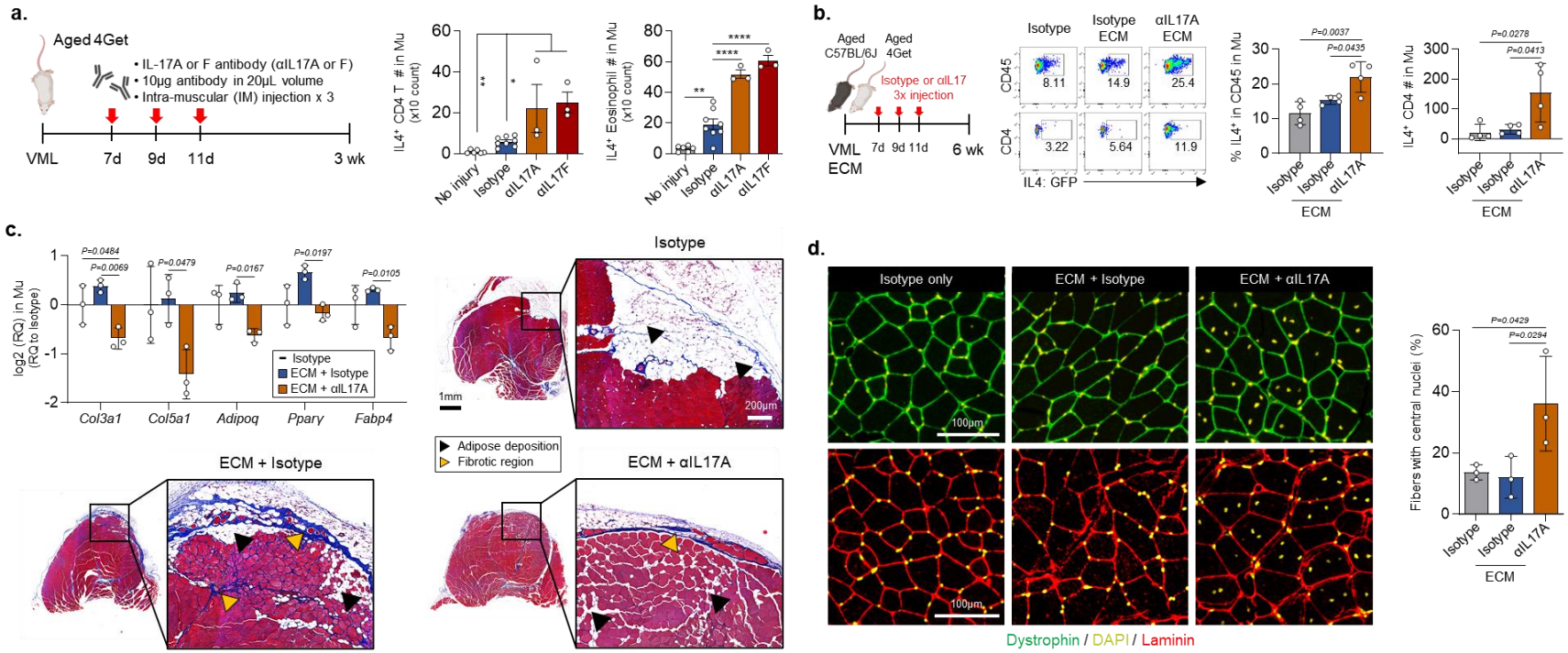

Figure 4. Local IL17 suppression rejuvenates the type 2 immune response to injury and ECM to restore tissue repair and reduce fibrosis in old animals. **a**, Schematic illustration of experimental design (left) and quantification of flow cytometry data for IL4$^+$ CD4 T cells and eosinophils in muscle 3 weeks after injury (right; n=6 no injury; n=8 isotype; n=3 αIL17A and αIL17F). **b**, Experimental schematics (left), and representative images flow cytometry showing IL4$^+$ CD45 or CD4 T cells (middle) and quantification of IL4$^+$ cell populations in muscle 6 weeks after injury and ECM treatment (right; n=4). **c**, Quantification of genes associated with fibrosis or adipogenesis in muscle (top left; n=3), and transverse section of the quadricep muscle 6 weeks after injury stained with Masson's Trichrome. **d**, Immunofluorescence images of the quadricep muscle 6 weeks after injury stained with dystrophin (top) or laminin (bottom). Quantification of muscle fibers with central nuclei are shown (right; n=3). Nuclei were stained with DAPI (represented in yellow). One-way ANOVA with Tukey's multiple comparisons test (**a-d**). *p<0.05, **p<0.01, and ****p<0.0001. For all bar graphs, data are mean ± s.e.m (**a**) or s.d. (**b-d**).